NOTES AND CORRESPONDENCE

The Spurious Production of Cloud-Edge Supersaturations by Eulerian Models

BJORN STEVENS, ROBERT L. WALKO, AND WILLIAM R. COTTON

Department of Atmospheric Science, Colorado State University, Fort Collins, Colorado

GRAHAM FEINGOLD

Cooperative Institute for Research in the Atmosphere, Colorado State University, Fort Collins, Colorado

25 April 1995 and 13 October 1995

ABSTRACT

The production of anomalous supersaturations at cloud edges other than cloud base has presented a vexing challenge for modelers attempting to represent the evolution of a droplet spectrum across an Eulerian grid. Although the problem manifests itself most dramatically for models that explicitly predict on the supersaturation field, it is also present in models with bulk condensation schemes in which condensation happens implicitly. Although the problem has been discussed in the context of truncation errors associated with finite difference approximations to advection, this note demonstrates more generally that the cloud-edge supersaturation problem is a fundamental problem associated with the ubiquitous assumption that the forcings on the droplet spectra are well represented by the mean thermodynamic fields. In certain respects, this assumption is equivalent to failing to represent fractional cloudiness within a grid. Although well-known consequences of this problem are the underprediction of temperature and the erroneous representation of the mean buoyancy flux within a grid box, we also demonstrate that the spurious production of droplets can arise in response to the spurious production of supersaturations in models with detailed microphysical representations.

1. Introduction

Over the past few years the cloud-edge supersaturation problem has presented a vexing challenge for two groups (e.g., Kogan et al. 1994 and Feingold et al. 1994) attempting to couple detailed representations of the droplet spectrum into large-eddy simulation (LES) dynamical models. In simulations of stratocumulus the cloud-edge supersaturation problem manifests itself at cloud top. Moreover, because of the strength of the inversion capping stratocumulus, the tendency toward nonmonotonic solutions using traditional higher-order advection operators is aggravated. In response to prior work, conservative thermodynamic variables and monotonic advection operators are generally used, but consistent with Grabowski's (1989) discussion of the problem, such an approach only mitigates the spurious production of cloud-top supersaturations. For instance, Fig. 1 is a snapshot of a typical supersaturation field produced in a simulation using conserved variables and monotonic advection operators. Although the model well represents the classical features of the supersaturation field, with cloud-base maxima falling off through the depth of the cloud, secondary cloud-top maxima remain as conspicuous and robust features of the simulations.

In numerical simulations of small cumulus in shear-free environments, Grabowski (1989) identified this problem of spurious supersaturations at cloud boundaries and noted that it intensified with increasing resolution. He also noted that monotonic corrections to the advective operators appear to mitigate the spurious supersaturation problem but do not eliminate it. This is because the cause of local extrema in supersaturations may be twofold: (i) the spurious generation of maxima and minima in the advective solutions of conserved thermodynamic variables can lead to spurious maxima and minima in the supersaturation field; and (ii) source terms in the supersaturation equation may generate local extrema. Physical sources of supersaturation exist only under vertical advection, perhaps prompting Grabowski (1989) to suggest that although monotonicity in the advection of thermodynamic fields guarantees monotonicity in the relative humidity field under horizontal advection, it is not sufficient to guarantee monotonicity in the relative humidity field under vertical advection. As we shall see, and as anticipated by Grabowski and Smolarkiewicz (1990; hereafter GS), there

Corresponding author address: Bjorn Stevens, Department of Atmospheric Science, Colorado State University, Fort Collins, CO 80523. E-mail: stevens@spot.atmos.colostate.edu

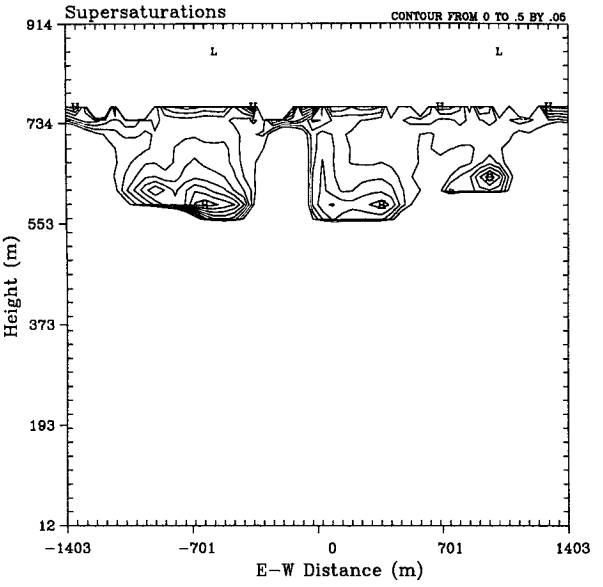

FIG. 1. A snapshot of the supersaturation field produced by a large-eddy simulation with explicit microphysics.

is a purely numerical source of supersaturations due to the ubiquitous assumption of homogeneity (i.e., the neglect of fractional cloudiness) on the grid scale. Because this source is not related to any physical process, but instead is related to the inability of most models to track cloud interfacial boundaries across a grid, it appears for both vertical and horizontal advection.

It is the purpose of this note to explore the impact of the assumption that forcings on the droplet spectra are well represented by the mean thermodynamic fields. It will be shown that such an assumption leads to the production of extrema in the temperature and supersaturation field along the boundaries of a cloud advecting across a fixed grid. Although the impact of neglecting fractional cloudiness on grid-averaged temperatures and buoyancy fluxes has long been recognized (e.g., Sommeria and Deardorff 1977), its impact on the supersaturation field and the resulting consequences for models that attempt to predict the evolution of the droplet spectrum has not been considered in detail. The rest of this note is organized as follows. In section 2 we develop a conceptual framework for the problem being considered. In section 3 we numerically investigate the hypothesis developed in section 2. Discussion proceeds in section 4, followed by conclusions in section 5.

2. A conceptual framework

The problem we are considering is the manner in which a specified spatial volume will change as a cloud advects through it. The resulting system of $N + 2$ equations, describing the time evolution of relevant filtered (or grid-scale variables) under constant isobaric advection and various forcings is just,

$$\frac{\partial \bar{\theta}_l}{\partial t} = -\bar{u}\frac{\partial \bar{\theta}_l}{\partial x} \tag{1}$$

$$\frac{\partial \bar{q}_w}{\partial t} = -\bar{u}\frac{\partial \bar{q}_w}{\partial x} \tag{2}$$

$$\frac{\partial \bar{r}_k}{\partial t} = -\bar{u}\frac{\partial \bar{r}_k}{\partial x} + \bar{\mathcal{F}} + \mathcal{F}', \quad \text{where} \quad k = 1, 2, \cdots, N, \tag{3}$$

and

$$\bar{\mathcal{F}} \equiv \mathcal{F}(\bar{\theta}_l, \bar{q}_w, \bar{r}_1, \cdots, \bar{r}_N; a_k) \quad \text{so that,}$$

$$\mathcal{F}' \equiv \mathcal{F}(\theta_l, q_w, r_1, \cdots, r_N; a_k) - \bar{\mathcal{F}}.$$

Where the overbar designates the filtered variables, θ_l is the liquid water potential temperature, and q_w is the total-water mixing ratio, both of which are conserved in the absence of precipitation. The forcing term on the radius of the kth aerosol category, r_k, is that due to condensation/evaporation and is denoted by $\mathcal{F}$. In addition to being a function of the prognostic variables, $\mathcal{F}$ has an implicit functional dependence on the ambient liquid water q_l and is parametrically dependent on the aerosol (assumed spherical and of some specified composition) dry radius denoted by a_k, and pressure, p_0. By choosing the number of aerosol categories, N, such that each category's number mixing ratio is unity, liquid water mixing ratio can be diagnosed from the above variables,

$$q_l = \frac{4}{3}\pi\rho_w \sum_k^N (r_k^3 - a_k^3), \tag{4}$$

where ρ_w the density of water is fixed and is not explicitly added to the argument set for $\mathcal{F}$. Consequently, specifying the set of fixed parameters $\{\bar{u}, p_0, a_k\}$ closes the system.

It is this filtered system of equation that best illustrates the current work, because it shows how three terms contribute to the microphysical evolution of the system. The first is the advection term, the second is the forcings associated with the filter-scale variables, and the last is the residual forcings, which generally involve correlations in subfilter variables.

There exist a variety of techniques available to solve a system of partial differential equations such as those described in Eqs. (1)–(3) above. One of the most common is the finite-difference approach whereby continuous derivatives are represented by finite difference analogs and the filter scale is taken to be the grid scale. In the presence of sharp gradients, finite difference approximations to the advection equation often result in significant truncation errors. Grabowski and Smolarkiewicz (1990) were primarily interested in how such truncation errors impacted the solutions to a simplified

form of the above system, where the simplification involved neglecting the detailed evolution of the cloud drop spectrum through the assumption that phase relaxation times were zero so that relative humidities never exceed unity, and all excess water was condensed. In contrast, our purpose is to assume that advection can be performed perfectly and examine the common assumption that $\mathcal{F}'$ is negligible in comparison to $\bar{\mathcal{F}}$. It will turn out that by formulating the problem in a simple enough way we are able to derive analytic solutions to the advective tendencies, thereby isolating the impact of approximations regarding the other forcings.

The assumption that $\mathcal{F}'$ is negligible compared to $\bar{\mathcal{F}}$ is common in Eulerian cloud models and is equivalent to assuming that the grid-averaged microphysics is well forced by the grid-averaged thermodynamics. In a sense, such an assumption is related to the neglect of fractional cloudiness, as cloud formation responds to whether or not the grid box is saturated in the mean. Some bulk condensation models have been formulated to account for fractional cloudiness (e.g., Sommeria and Deardorff 1977). Although such methods may facilitate the computation of the $\mathcal{F}'$ term above, when such approaches are taken, it is generally in models with larger grid volumes and for purposes other than accurately representing the forcings on the grid-scale droplet spectrum. To our knowledge every model that represents the explicit evolution of the cloud drops does so on a relatively small grid scale and so it has been universally assumed that neglect of higher-order terms, and the resulting neglect of $\mathcal{F}'$, is justified.

Let us first heuristically understand the evolution of the system described by Eqs. (1)–(3). Using the cartoon depicted in Fig. 2, the essence of the problem is illustrated in terms of a three-step process. To begin with (i.e., for $t < \tau^*$; where τ^* is the time at which the grid box saturates in the mean) the mean relative humidity of the downwind grid box will increase because of the changing temperature and moisture under advection. How fast the relative humidity increases depends on the partitioning of the total water between the vapor and liquid forms. So long as the grid-averaged relative humidity is less than 100% and the advection timescales are greater than the evaporation timescales, cloud drops that are independently advected into the grid box will be evaporated and deactivated. Because of this evaporation of liquid water, the vapor field builds too rapidly, and the sensible temperature field decreases, causing relative humidities to rise too rapidly. This process proceeds until some time $t = \tau^*$ at which the downwind grid box becomes just saturated and cloud drops will no longer evaporate upon being advected into it. During the first interval, $t \in (0, \tau^*)$, some fraction less than τ^*/τ of drops will evaporate. However, during the second interval, $t \in (\tau^*, \tau)$, where τ is the advective timescale, the formerly dry grid box must begin to recondense the water and reactivate the drops that were evaporated in the first half of the process. If the timescales for this process are sufficiently long, the downwind grid box may recondense the water without reactivating any of the drops that were evaporated during the first half of the process. If the timescales are too short, reactivation may occur. In both cases the situation is such that the final drop concentrations in the downwind grid box may only bear a weak relation to the concentrations originally present in the upwind or donor grid cell. Consequently, we may see a reduction in the number of drops associated with a spuriously low cloud-top supersaturation, or an enhancement, solely as a product of the timescale τ of the advection. One mitigating factor would be that in the absence of strong gradients in relative humidity across the cloud boundary, the evaporation timescales may be longer than the advective timescales; consequently, sufficient integral radius may remain so as to prevent spurious reactivation during the time period over which recondensation takes place.

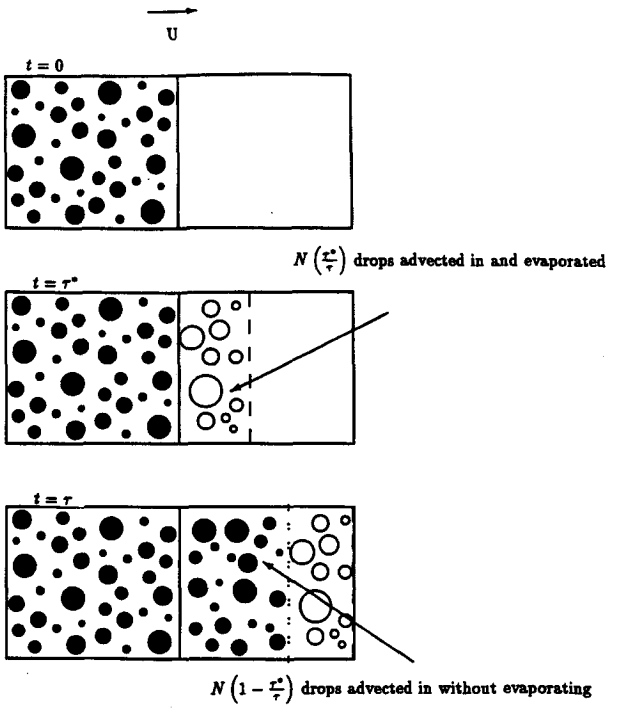

FIG. 2. Schematic representation of the movement of a cloud boundary across a grid under constant, isobaric flow.

3. Numerical investigations of conceptual model

The numerical problem is formulated in an idealized manner to more clearly illustrate its essence. Specifically, we shall constrain our cloud and environment to both be steady and horizontally homogeneous in subdomains, which are respectively described by the constant vectors $\chi^{(c)}$ and $\chi^{(e)}$. Where χ is used to represent the set of prognostic variables:

$$\chi = \{\theta_l, q_w, r_1, \cdots, r_N\}. \quad (5)$$

The dry aerosol size distributions are considered constant across the entire domain and are initialized as in Stevens et al. (1996).

The cloud, $\chi^{(c)}$, is initialized to be exactly saturated at some equilibrium liquid water content with some number of activated aerosol categories N_a, such that the fraction of activated aerosol is given by $N_a/N < 1$. The environment, $\chi^{(e)}$, is initialized at some relative humidity less than one, with the radius of the aerosol corresponding to their equilibrium sizes. The cloud boundary is initially coincident with a grid boundary, and the flow velocity and grid scale are implicitly specified through an advective timescale τ, which represents the amount of time it takes a cloud to transverse a grid cell. We will be interested in the evolution of the state of a grid cell described by $\bar{\chi}(t)$ as a function of time $t \in (0, \tau)$.

The analytic solution is such that $\bar{\chi}$ changes linearly from $\chi^{(e)}$ to $\chi^{(c)}$ over the interval, in response to the

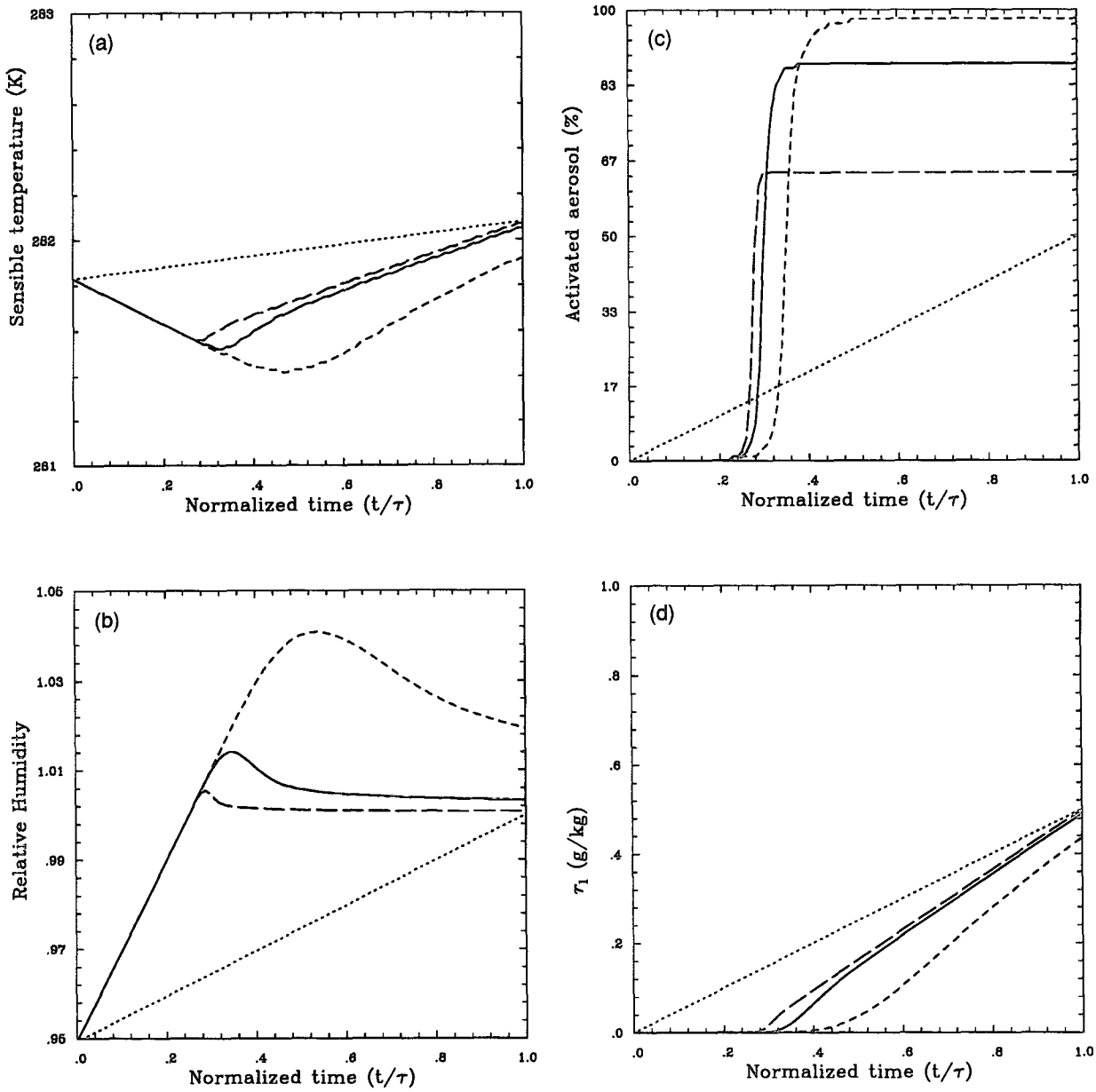

FIG. 3. Evolution of various fields as a function of normalized time, t/τ, for three different values of τ. Analytic solutions are given by linear dotted line. Solid line corresponds to $\tau = 181$, short dash corresponds to $\tau = 32$, long dash corresponds to $\tau = 1024$. Sensible temperature (a); relative humidity (b); percent of activated aerosol (c); and liquid water mixing ratio (d).

advective tendencies and the lack of any physical forcings on the droplet spectrum (i.e., $\mathcal{F} = 0$). In other words, at any time in the interval $(0, \tau)$ the grid volume will be composed of a fraction t/τ of cloudy air described by $\chi^{(c)}$, and the remainder of the volume will be environmental air. Consequently the analytic solution of the evolution of $\chi(t)$ is simply the linear combination of cloudy and environmental states:

$$\bar{\chi}(t) = \begin{cases} \chi^{(e)}, & t < 0 \\ \chi^{(e)} + \dfrac{\chi^{(c)} - \chi^{(e)}}{\tau} t, & 0 \leq t \leq \tau \\ \chi^{(c)}, & t > \tau \end{cases} \quad (6)$$

For steady isobaric advection $\mathcal{F} = 0$, and the analytic solution to the advective tendencies is given by taking the time derivative of the above solution:

$$\left[\frac{d\bar{\chi}(t)}{dt}\right]_{\text{adv}} = \frac{\chi^{(c)} - \chi^{(e)}}{\tau}, \quad \text{for} \quad 0 \leq t \leq \tau. \quad (7)$$

The system may be numerically integrated, using the analytic solution to the advective tendency over the interval $(0, \tau)$ given by Eq. (7), to see how the microphysical fields respond under the assumption that $\mathcal{F}'$ is negligible. Because there are no forcings (in the Lagrangian sense) on θ_l or q_w, the procedure formally guarantees the correct time evolution for these variables, reducing the problem to one of integrating the following set of ordinary differential equations over the interval $(0, \tau)$ and under the assumption that $\mathcal{F}'$ is negligible:

$$\frac{d\bar{\theta}_l}{dt} = \frac{\theta_l^{(c)} - \theta_l^{(e)}}{\tau} \quad (8)$$

$$\frac{d\bar{q}_w}{dt} = \frac{q_w^{(c)} - q_w^{(e)}}{\tau} \quad (9)$$

$$\frac{d\bar{r}_k}{dt} = \frac{r_k^{(c)} - r_k^{(e)}}{\tau} + \bar{\mathcal{F}}, \quad \text{where} \quad k = 1, 2, \cdots, N. \quad (10)$$

By considering the evolution of a single grid box, the x dependence of the system has been eliminated through the specification of the analytic solutions to the advective tendencies and the partial time derivatives are replaced by total time derivatives. The integration is performed in two parts, as the advective tendencies are first applied at each time increment using a forward timestep, the forcing terms are subsequently integrated on the same small timestep using the differential equation solver VODE (Brown et al. 1989). The integration has been done at increasingly small time increments to ensure convergence of the solutions.

In Fig. 3 a number of fields are plotted as a function of nondimensionalized time, t/τ. The analytic solutions are given by the dotted line, whereas the numerical solutions are realized by driving the microphysical forcings with the grid-averaged supersaturation field in the manner described above. The solid line is the control corresponding to a timescale of $\tau = 181$ s, the long-dashed line corresponds to a longer timescale of $\tau = 1024$ s, while the short-dashed line corresponds to a shorter timescale of $\tau = 32$ s. Values of the initial state are tabulated in Table 1.

These results demonstrate our earlier arguments, whereby nonmonotonic behavior is observed in the sensible temperature (Fig. 3a) and the relative humidity (Fig. 3b) as a byproduct of driving the microphysical forcings with the grid-averaged values of the supersaturation field. Initially, the grid is on average subsaturated, so that the number of activated aerosol (Fig. 3c) is zero, as all the drops advected in to the grid box are promptly evaporated; correspondingly, there is no liquid water in the domain (Fig. 3d), and sensible temperatures are depressed from what they should otherwise be. At some time, actually prematurely, the grid becomes saturated in the mean. However at this time there are no previously activated drops present to accommodate the production of excess vapor, nor is the liquid water that is being advected-in sufficient to accommodate the rapid rate of vapor production. Consequently, supersaturations develop [of the order of several percent consistent with the simulations of Grabowski (1989)] and droplet activation from the ambient aerosol population proceeds. Shortly thereafter, supersaturations peak and then begin falling again as sufficient integral radius is available to accommodate the ambient excess vapor and its continual production. At this point, further activations cease (Fig. 3c), and temperatures begin to converge on the analytic solutions from below (Fig. 3a).

Notice that during the course of this process the sensible temperature and supersaturation both develop local extrema (i.e., they are nonmonotonic) and that this property is not a result of truncation errors in the advection of prognostic variables, but rather a logical consequence of driving microphysical forcings with grid-averaged supersaturations. In addition, comparing the curves within Fig. 3a and Fig. 3b it is apparent that the extent of the local extrema in the relative humidity and sensible temperature fields is a function of the timescale of the process. Shorter timescales favor larger supersaturations, which lead to more activated aerosol and smaller mean diameters. Larger supersaturations on shorter timescales is a result consistent with Grabow-

TABLE 1. Values of environmental and cloudy states at initial time.

	θ_l (K)	q_w (g kg^{-1})	q_l (g kg^{-1})	N_a/N (%)
$\chi^{(c)}$	285.3	8.0	0.5	50
$\chi^{(e)}$	286.3	7.0	0.0	0

Pressure was held constant at $p_0 = 946$ mb.

ski's (1989) observations of increasing supersaturations at cloud edges due to a reduction in grid spacing, although his results also showed the effect of the increasing truncation error associated with imperfect finite difference approximations to advection.

To better illustrate the manner in which timescales impact the solutions we repeated our simulations for several more advective timescales and plotted the number of activated drops corresponding to $\overline{\chi}(t = \tau)$ versus τ in Fig. 4. The results illustrate the earlier arguments that postulated that the number of drops at the end of the advection process will be a strong function of the timescale of the advection. Moreover, it appears that the actual number of activated drops at the end of the process is relatively independent of the analytic answer.

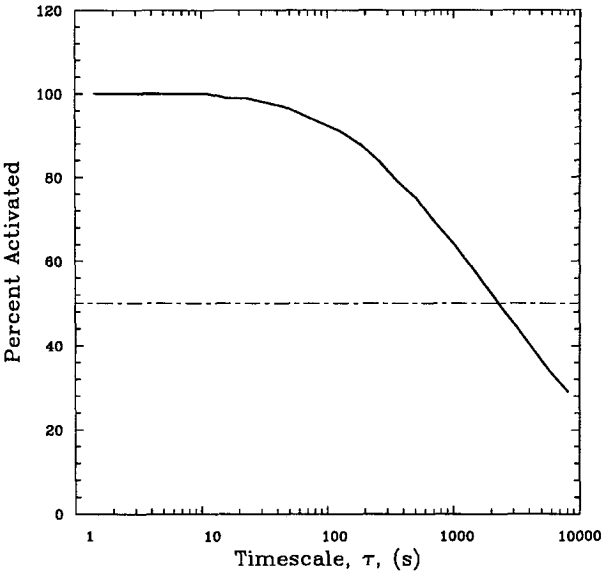

FIG. 4. Variation of percent of activated drops as a function of timescale τ. The analytic solution would be independent of timescale with $N_a/N = 50\%$.

4. Discussion

In analyzing problems similar to that discussed here, GS recognized that viscous mixing between cloud and subsaturated air could generate cooling due to the evaporation of cloud drops and conjectured that even in the strictly inviscid sense undershoots in the potential temperature could occur at the cloud edges because of the inability of models to "track the actual position of the cloud boundary within a grid box." However, as discussed in section 2, their work was primarily concerned with addressing how truncation errors in solutions to the advection equation impacted the monotonicity of the supersaturation field. In one extension of the flux-limiting methodology, they did, however, attempt to limit extrema in the supersaturation field, by placing extra limiters on the total water field. However, having herein demonstrated their conjecture (i.e., that the local extrema in potential temperature and hence supersaturation is related to the failure to track cloud interfacial boundaries through a grid box) one may question the benefit of forcing monotonicity, through limiters applied to the advective operators, on a field whose source of local extremum is, at least in part, related to a process other than advection. In other words, it does not seem appropriate (as in GS) to ensure monotonicity in the supersaturation field by applying additional[1] corrections to the advective representation of the basic thermodynamic variables.

The results reported above suggest that a basic problem in representing the supersaturation field in an Eulerian model stems from the inability to represent the location of the boundary of the cloud with a resolution better than the model grid scale. Although it was shown that the inability to locate the boundary of the cloud within a grid box is equivalent to the inability to represent subgrid variability in the condensational forcing terms of models with detailed microphysics, even in bulk models where the forcing is implicit (through the transcendental equation relating θ to θ_l and q_w), this problem will persist as long as the implicit relations are based on grid-averaged variables only.

Although underestimates in the temperature and overestimates in the negative buoyancy flux are problems associated with both bulk and detailed microphysical models, these problems of fractional cloudiness have been discussed in the past. Given that, the principle contribution of the present work is to illustrate the manner in which the fractional cloudiness problem impacts models that (in predicting the supersaturation field) predict the detailed evolution of the droplet spectrum. Our results suggest that over large areas of the cloud boundary, the spurious generation of supersaturations will lead to the activation of aerosol in a manner that bears little or no relationship to the activation of aerosol associated with cloud-base supersaturations in ascending air. Consequently, in the absence of either a resolution to this problem, or ingenious sensitivity experiments, modelers who use detailed microphysics to evaluate a number of mixing hypotheses will be unable to state with confidence to what extent the droplet spectra, which results from mixing across cloud interfacial boundaries, will accurately represent the physical system.

The quantitative extent of these problems will likely be a function of the rate at which a cloud moves across a grid, in addition to the amount of cloud surface area

[1] Additional in the sense that they do more than ensure monotonicity in the advected field, but also ensure monotonicity in other secondary fields whose departures from monotonicity are not related to errors in the representation of advection in the primary thermodynamic fields.

relative to volume. Consequently, simulations of relatively shallow cumulus that move across a grid in a mean wind would appear to be particularly susceptible to the sorts of problems discussed here. For simulations of stratocumulus in which the cloud is relatively well capped, and cyclical in the horizontal, problems are limited to cloud top. In particular it appears that the descent of the cloud top, near the region feeding a downdraft, causes the grid box to become subsaturated in the mean, leading to the premature evaporation of cloud drops. As a consequence, the number concentrations in downdrafts are significantly depleted (Stevens et al. 1996). This indicates how the problem, which hitherto has been discussed in the simple case of the leading edge of a cloud advecting into a formerly dry grid box, is also significant along the trailing edge of the cloud.

Despite strong evidence that simulated cloud-top supersaturations are a numerical artifact, certain physical explanations have been advanced and may be worthy of further exploration. Kogan et al. (1994) suggested that strong radiative cooling at cloud top could be responsible for the observed cloud-top maxima in the supersaturation field. Simulated cooling rates on the order of 10 K h^{-1} are equivalent to the expansional cooling associated with updraft velocities on the order of 0.5 m s^{-1} and could at first glance constitute a significant forcing on the supersaturation field. However, such affects are not consistent with short-phase relaxation times at cloud top. Additionally, gravity waves have been posited as a forcing for cloud-top supersaturations (Kogan et al. 1995). Here the proposed mechanism has mixing causing an evaporation of all liquid water in a parcel so that the parcel resides just below its lifting condensation level. Acted upon by gravity waves, these just subsaturated parcels of air may be sharply forced above their lifting condensation level forcing the generation of supersaturations and the reactivation of drops within the parcel for entirely physical reasons. Although it is conceivable that physical processes (such as the collusion of events in the gravity wave hypothesis) may lead to the production of cloud top supersaturations, it is our belief that the numerical issues discussed above obviate our ability to discuss hypotheses such as these on the basis of results from the current generation of numerical models—particularly because gravity waves will increase vertical velocities at cloud top, exacerbating the numerical problems.

Although it is not the purpose of this note to consider solutions to the above problems, some comments in this respect are in order. The fractional cloudiness scheme developed by Sommeria and Deardorff (1977) allows the diagnosis of fractional cloud amount R and mean liquid water $\bar{q}_l$ within a grid cell, based on the assumption that the total water q_w and liquid water potential temperature θ_l are distributed according to a bivariate Gaussian distribution function. Such a scheme relies on some information about the covariances and variances of the thermodynamic set $\{q_w, \theta_l\}$, and these may be obtained either by solving prognostic equations for the variance or diagnosing them assuming quasi-stationary statistics. In either case, information about the set $\{R, \bar{q}_l, \bar{q}_w, \bar{\theta}_l, \overline{\theta_l'\theta_l'}, \overline{q_w'q_w'}\}$ could conceivably be used to partition a grid cell into cloudy and clear states denoted by the variable set $\{R, \bar{q}_l, \bar{q}_w^c, \bar{\theta}_l^c, \bar{q}_w^e, \bar{\theta}_l^e\}$, such that the variances and means are preserved. The microphysics could be forced on this partitioned grid, perhaps alleviating the problems discussed above. An alternative method that shows promise is one in which the volume of cloud is tracked within the grid box. This allows for the reconstruction of the cloud boundary and the partitioning of physical processes into the cloudy and noncloudy subdomains. Although there are a number of algorithms designed for tracking the motion of an interfacial surface across a three-dimensional grid, the volume-of-fluid method (VOF) appears quite promising because it represents the best trade-off between efficiency and accuracy; currently it is being implemented and tested in two-dimensional cloud models (J. Reisner 1995, personal communication).

5. Conclusions

The inability of models to accurately track the cloud boundary within a grid box leads to spurious production or destruction of cloud drops at leading and trailing edges of a cloud. Formally this problem can be thought of one in which the neglect of subgrid variability in the microphysical forcings has serious implications on the evolution of the cloud as it moves across a discretized domain. A component of this problem is the underprediction of liquid water in partially filled grid boxes, which results in underpredictions of temperature and buoyancy forces in those grid boxes. Although these artifacts were demonstrated in the context of detailed microphysical models, they will also be evident in bulk microphysical models and could impact the ability of cloud models to accurately address a variety of hypotheses associated with mixing across cloud interfacial boundaries.

Acknowledgments. Bjorn Stevens is thankful for his funding under a NASA/EOS Global Change Fellowship and also gratefully acknowledges discussions with Chin-Hoh Moeng and Wojciech Grabowski that helped clarify certain issues. Suggestions by Wojciech Grabowski's and an anonymous reviewer also led to improvements in this notes presentation. Piotr Smolarkiewicz and Craig Tremback are thanked for their help with the flux-corrected transport methodology. Thanks also to our sponsors, the U.S. Department of Energy, Contract DE-FG03-94ER61749 and the National Institute for Global Environmental Change, Research Agreement Number NIGEC-91-S01.

REFERENCES

Brown, P. N., G. D. Byrne, and A. C. Hindmarsh, 1989: VODE: A variable coefficient ODE solver. *SIAM J. Sci. Stat. Comput.*, **10,** 1038–1051.

Feingold, G., B. Stevens, W. R. Cotton, and R. L. Walko, 1994: An explicit cloud microphysics/LES model designed to simulate the Twomey effect. *Atmos. Res.*, **33,** 207–233.

Grabowski, W. W., 1989: Numerical experiments on the dynamics of the cloud-environment interface: Small cumulus in a shear free environment. *J. Atmos. Sci.*, **46,** 3513–3541.

——, and P. K. Smolarkiewicz, 1990: Monotone finite-difference approximations to the advection–condensation problem. *Mon. Wea. Rev.*, **118,** 2082–2097.

Kogan, Y. L., D. K. Lilly, Z. N. Kogan, and V. V. Filyushkin, 1994: The effect of CCN regeneration on the evolution of stratocumulus cloud layers. *Atmos. Res.*, **33,** 137–150.

——, M. F. Khairoutdinov, D. K. Lilly, Z. N. Kogan, and Q. Liu, 1995: Study of the effects of stratocumulus cloud layer dynamics on microphysics using a three-dimensional large-eddy simulation model with explicit microphysics. *Proc. Conf. on Cloud Physics,* Dallas, TX, Amer. Meteor. Soc., 165–170.

Sommeria, G., and J. W. Deardorff, 1977: Subgrid-scale condensation in models of non-precipitating clouds. *J. Atmos. Sci.*, **34,** 344–355.

Stevens, B., G. Feingold, W. R. Cotton, and R. L. Walko, 1996: Elements of the microphysical structure of numerically simulated nonprecipitating stratocumulus. *J. Atmos. Sci.*, **53,** 980–1006.